The relationship between intranuclear mobility of the NF-kappa B subunit p65 and its DNA binding affinity

Schaaf, M.J.J.; Willetts, L.; Hayes, B.P.; Maschera, B.; Stylianou, E.; Farrow, S.N.

THE JOURNAL OF BIOLOGICAL CHEMISTRY VOL. 281, NO. 31, pp. 22409–22420, August 4, 2006

The Relationship between Intranuclear Mobility of the NF-κB Subunit p65 and Its DNA Binding Affinity*

Received for publication, October 12, 2005, and in revised form, June 6, 2006 Published, JBC Papers in Press, June 7, 2006, DOI 10.1074/jbc.M511086200

Marcel J. M. Schaaf[‡1], **Lynsey Willetts**[‡§2], **Brian P. Hayes**[‡], **Barbara Maschera**[‡], **Eleni Stylianou**[§], **and Stuart N. Farrow**[‡]

From the [‡]*Department of Asthma Biology, GlaxoSmithKline, Gunnels Wood Road, Stevenage, Hertfordshire SG1 2NY and* [§]*School of Biomedical Sciences, University of Nottingham, Queen's Medical Centre, Nottingham NG7 2UH, United Kingdom*

It has been hypothesized that the main determinant of the intranuclear mobility of transcription factors is their ability to bind DNA. In the present study, we have extensively tested the relationship between the intranuclear mobility of the NF-κB subunit p65 and binding to its consensus target sequence. The affinity of p65 for this binding site is altered by mutation of specific acetylation sites, so these mutants provide a model system to study the relationship between specific DNA binding affinity and intranuclear mobility. DNA binding affinity was measured *in vitro* using an enzyme-linked immunosorbent assay-based method, and intranuclear mobility was measured using the fluorescence recovery after photobleaching technique on yellow fluorescent protein-tagged p65 constructs. A negative correlation was observed between DNA binding affinity and intranuclear mobility of p65 acetylation site mutants. However, moving the yellow fluorescent protein tag from the C terminus of p65 to the N terminus resulted in an increased mobility but did not significantly affect DNA binding affinity. Thus, all changes in DNA binding affinity produce alterations in mobility, but not *vice versa*. Finally, a positive correlation was observed between mobility and the randomness of the intranuclear distribution of p65. Our data are in line with a model in which the intranuclear mobility and distribution of a transcription factor are determined by its affinity for specific DNA sequences, which may be altered by protein-protein interactions.

Using the fluorescence recovery of photobleaching (FRAP)[3] technique on green fluorescent protein-tagged proteins in living cells, it has become possible to monitor the mobility of proteins *in vivo*. The first reports on the dynamics of nuclear proteins revealed a remarkably high mobility for a variety of nuclear proteins, such as the endonuclease ERCC1/XPF (1), the nucleosomal binding protein HMG-17, the pre-mRNA splicing factor SF2/ASF, and the rRNA processing protein fibrillarin (2). More information on the regulation of the mobility of nuclear proteins has come from studies on steroid receptors, which act as transcription factors upon activation by their ligand. It was shown for estrogen receptor α (3–5), the glucocorticoid receptor (GR) (6, 7), and the androgen receptor (8) that activation by ligand decreases the mobility of the receptor and that the ligand-binding domain and DNA-binding domain are important for this effect. In addition, for GR, it was shown that regional differences in mobility occur, with the lowest mobility found in regions with the highest concentration of receptors (9).

It is commonly believed that transcription factors in the nucleus freely diffuse between sites to which they transiently bind (7, 10). The association with these binding sites is suggested to be the most important determinant of the average transcription factor mobility in the nucleus as measured by FRAP. The nature of these sites has not yet been elucidated, but it has been suggested that DNA binding is the main determinant of transcription factor mobility in the nucleus (7, 10). Recent studies using the ChIP-chip technology have revealed a surprisingly high number of p65 DNA-binding sites in the human genome (~20,000) (11). Of these sites, 35% contain a canonical p65 target sequence, whereas the other 65% probably reflect sites at which p65 binds through interaction with other proteins that associate with specific DNA sites. Only one-third of the p65 binding sites were found within 5 kb upstream of a transcription start site, and 38% of the binding sites lie near or within genes that are not regulated after activation of p65 by tumor necrosis factor α (11). Thus, the function of a majority of p65 binding sites remains to be elucidated. Similarly high numbers of binding sites have been found for SP-1, c-Myc, CREB, and E2F1, also by application of the ChIP-chip technology (12–14).

Because of this high number of transcription factor DNA-binding sites, we hypothesize that association with DNA determines the intranuclear mobility of transcription factors. Indeed, deletion of the DNA-binding domain of GR (6) and the yeast transcription factor Ace1p (15) and a point mutation in the androgen receptor DNA-binding domain (8) result in increased mobility of the protein. These deletions, however, were relatively large, which could result in alterations in the conformation of other domains of the protein or misfolding. For example, for GR, it was found that deletion of the DNA-

* The costs of publication of this article were defrayed in part by the payment of page charges. This article must therefore be hereby marked "*advertisement*" in accordance with 18 U.S.C. Section 1734 solely to indicate this fact.

[1] Supported by European Union Marie Curie Industry Host Fellowship E2603. To whom correspondence should be addressed: Institute of Biology, Clusius Laboratory, Leiden University, Wassenaarseweg 64, 2333 AL Leiden, The Netherlands. Tel.: 31-71-5274975; Fax: 31-71-5275088; E-mail: schaaf@rulbim.leidenuniv.nl.

[2] Supported by an Engineering and Physical Sciences Research Council/GlaxoSmithKline Cooperative Award Ph.D. studentship.

[3] The abbreviations used are: FRAP, fluorescence recovery of photobleaching; GR, glucocorticoid receptor; ChIP-chip, chromatin immunoprecipitation-microarray analysis; EMSA, electrophoretic mobility shift assay; IL, interleukin; CV, coefficient of variation; ANOVA, analysis of variance; YFP, yellow fluorescent protein; ELISA, enzyme-linked immunosorbent assay; CREB, cAMP-response element-binding protein; CBP, CREB-binding protein.

binding domain results in a protein that forms aggregates in the nucleus and cytoplasm, which probably reflects accumulations of misfolded proteins (9). Furthermore, the mutation described above resulted in loss of DNA binding, and the effect of increasing the DNA binding affinity has not been studied.

In the present study, we have extensively tested the relationship between intranuclear mobility and specific DNA binding, using the NF-κB subunit p65 as a model system. NF-κB plays a central role in induction of genes that are involved in immune and inflammatory responses (16, 17). The prototypical NF-κB is a p50/p65 heterodimer, but p65 homodimers occur and are functional as well (18). NF-κB is sequestered in the cytoplasm by its inhibitor IκB, which in response to inflammatory stimuli is phosphorylated and targeted for degradation by the proteasome in response to inflammatory stimuli (17). NF-κB subsequently translocates to the nucleus and transactivates target genes.

Acetylation of p65 *in vivo* appears to be a mechanism for regulation of its transcriptional activity (19, 20). Five lysine residues can be targeted for acetylation: Lys-122, Lys-123, Lys-218, Lys-221, and Lys-310. The crystal structure of a p65/p50 heterodimer bound to the κB site of the immunoglobulin light chain gene promoter demonstrates that the first four residues contact the DNA backbone, whereas Lys-310 is not involved in DNA binding (21, 22). Residues Lys-122 and Lys-123 can be acetylated by p300 and p300/CBP-associated factor, which decreases the DNA binding affinity of p65 as demonstrated by electrophoretic mobility shift assay (EMSA) (23). Acetylation of Lys-218 and Lys-221 can occur through p300 and CREB-binding protein (but not p300/CBP-associated factor), resulting in increased DNA binding affinity, also demonstrated by EMSA (24, 25). Acetylation of Lys-310 does not alter DNA binding but does increase the transcriptional activity of p65, probably by increasing the affinity for a transcriptional coactivator (24, 25). Mutating these lysine residues to arginine prevents acetylation of the amino acid but retains the positive charge of this residue. In contrast, mutation to alanine neutralizes the positive charge, thereby mimicking this effect of acetylation.

It has been shown that by introducing these mutations into p65, it is possible to either increase or decrease its binding affinity for the κB consensus sites (23–25). These mutants then provide a model system that can be exploited to test the relationship between specific DNA binding affinity and intranuclear mobility. Using this approach, in the present study, a clear relationship was observed between DNA binding and intranuclear mobility. However, comparison between p65 that was N-terminally tagged with yellow fluorescent protein (YFP) and p65 C-terminally tagged with YFP demonstrates that DNA binding affinity is not the sole determinant of intranuclear mobility of transcription factors and that additional factors like interaction with other nuclear proteins may also alter mobility.

EXPERIMENTAL PROCEDURES

Plasmids—Synthesis of the expression plasmid pp65-EYFP, encoding p65 with YFP tagged at its C terminus, was described previously (26). Briefly, the p65 coding sequence was subcloned from plasmid pp65-EGFP (construction described by Nelson *et al.* (27)) into pEYFP-N1 (Clontech) using HindIII and BamHI restriction sites.

The expression plasmid pEYFP-p65, encoding p65 with YFP tagged at its N terminus, was constructed by PCR amplification of the p65 coding sequence from the expression vector pCMV4-p65 (28). The primer sequences used were GATTAGGATCCGACGAACTGTTCCCC CTCATC (containing the BamHI site and removing the ATG from p65) and CTATAGAATAGGGCCCTCTAGATGCATGCTCG (containing the XbaI site). The PCR product was cloned into the vector pEYFP-C1 (BD Biosciences Clontech) by using BamHI and XbaI restriction sites.

Mutated versions of this vector were made by site-directed mutagenesis using the QuikChange kit (Stratagene) according to the manufacturer's instructions. For expression of nontagged p65, a stop codon was introduced into the plasmid pp65-EYFP immediately behind the p65 coding sequence using site-directed mutagenesis. All plasmids were verified by sequence analysis. Wild type p65 sequence was identical to the previously described sequence (29).

For reporter assays, pNF-κB-Luc (Stratagene) was used, which contains five repeats of an NF-κB-sensitive enhancer element (TGGGGACTTTCCGC) upstream of the TATA box, controlling the expression of luciferase. The empty expression vector pcDNA3 (containing a cytomegalovirus promoter like pp65-EYFP and pEYFP-p65) was used as a control for the amount of DNA.

Cell Culture and Transfection—COS-1 cells were grown as described previously (9). Transfections were performed using Fugene 6 (Roche Applied Science) according to the manufacturer's instructions. A Fugene/DNA mixture was made in Opti-MEM (Invitrogen) as indicated for each experiment. Cells were incubated with this mixture for 5 h at 37 °C and refed with supplemented Dulbecco's modified Eagle's medium.

Luciferase Reporter Assays—Cells were plated in 9.6-cm^2 wells (1.5×10^5 cells/well) 1 day before transfection. Each well was transfected using 3 μl of Fugene 6, 0.5 μg of the reporter plasmid pκB-luc, and the indicated amounts of p65 or YFP-tagged p65 expression vector or a mutated version of one of these vectors. The total amount of transfected DNA was kept at 1.5 μg by adding pcDNA3. Twenty-four hours after the start of the transfection, cells were trypsinized and plated in 96-well plates (50×10^3 cells/well). Each individual transfection was plated in duplicate. After incubation at 37 °C for 6 h, luminescence was measured using the Firelite dual luminescence reporter gene assay system (PerkinElmer Life Sciences). Luminescence was read on a Wallac 1450 Microbeta Trilux luminescence counter (PerkinElmer Life Sciences). In each experiment, duplicates were averaged. Data shown are average ± S.E. of at least three individual experiments.

Western Blots—Aliquots of each nuclear extract were analyzed by Western blotting. Using 8% polyacrylamide gels (Invitrogen), 5 μg of protein was resolved by electrophoresis, and samples were subsequently transferred electrophoretically to nitrocellulose membranes (Invitrogen). Membranes were blocked at room temperature for 30 min in Tris-buffered saline with Tween 20 (TBST; 10 mM Tris-HCl (pH 7.4), 150 mM NaCl, and 0.1% Tween 20) containing 5% nonfat dry milk. Subse-

quently, the membrane was incubated overnight at 4 °C with either the p65 antibody (C-20 (Santa Cruz Biotechnology, Inc., Santa Cruz, CA)) or the green fluorescent protein antibody (FL (Santa Cruz Biotechnology)) at a dilution of 1:1000 or 1:200, respectively in TBST containing 5% nonfat dry milk. After three 15-min washes in TBST containing 5% nonfat dry milk, the membrane was incubated with a horseradish peroxidase-labeled goat anti-rabbit secondary antibody (Amersham Biosciences; 1:2000 dilution in TBST containing 5% nonfat dry milk) for 1.5 h at room temperature. Finally, after three 15-min washes in TBST, immunoreactivity was visualized by enhanced chemiluminescence (ECL; Amersham Biosciences) according to the manufacturer's instructions.

NF-κB DNA Binding Assay—Cells were plated in 78.5-cm^2 dishes (7.5×10^5 cells/dish) 1 day before transfection. For transfection, 15 μl of Fugene and 5 μg of pp65-YFP or a mutated version of this vector was used per dish. One day later, nuclear extracts were prepared using a method established by Andrews and Faller (30). Cells were scraped off in 1 ml of ice-cold phosphate-buffered saline, spun down (1 min, 13,000 rpm, 4 °C), and resuspended in 200 μl of buffer A (10 mM Hepes-KOH, pH 7.9, at 4 °C, 1.5 mM $MgCl_2$, 10 mM KCl, 0.5 mM dithiothreitol, Protease Inhibitor Mixture Set III (1:1000; Calbiochem)). Cells were incubated on ice for 10 min, vortexed for 10 s, and spun down (1 min, 13,000 rpm, 4 °C). The pellet was resuspended in 200 μl of buffer C (20 mM Hepes-KOH, pH 7.9, 25% glycerol, 420 mM NaCl, 1.5 mM $MgCl_2$, 0.2 mM EDTA, 0.5 mM dithiothreitol, Protease Inhibitor Mixture Set III (1:1000; Calbiochem)) and incubated on ice for 20 min. After centrifugation (2 min, 13,000 rpm, 4 °C), supernatants were collected and stored at −20 °C.

DNA binding affinity was measured using the TransAM NF-κB Chemi kit (Active Motif) according to the manufacturer's instructions. Serial dilutions (1:2) were made of the nuclear extracts, and 20 μl of each dilution and 30 μl of binding buffer were added to a microtiter plate coated with an oligonucleotide containing the κB site of the immunoglobulin light chain gene promoter (GGGACTTTCC). After incubation at room temperature for 1 h, wells were washed three times in 200 μl of washing buffer. Subsequently, wells were incubated with NF-κB antibody (1:1000) for 1 h and were washed three times in washing buffer. After a 1-h incubation with horseradish peroxidase-conjugated secondary antibody (1:10,000), wells were washed four times, chemiluminescent substrate was added, and luminescence was measured using a Wallac 1450 Microbeta Trilux luminescence counter (PerkinElmer).

In order to measure relative p65-YFP protein levels in the nuclear extracts, the yellow fluorescence in the nuclear extracts was measured using a Wallac 1420 multilabel counter, using excitation at 485 nm and a 535-nm long pass filter for the emission (PerkinElmer Life Sciences). In a control experiment, it was verified that the YFP concentration in the sample was proportional to the measured fluorescence level. Fluorescence levels were corrected for total protein concentration in the sample, and subsequently the luminescence levels from the DNA binding assay were plotted against the fluorescence level. From these curves, the EC_{50} values were calculated for each mutant. In each experiment, EC_{50} values were corrected for the EC_{50} of p65-YFP, which was set at 100%. Data shown are average ± S.E. of at least three individual experiments. Statistical analysis of these experiments was performed on log-transformed data.

Interleukin-8 (IL-8) Immunoassay—Quantitative determination of IL-8 concentrations in cell culture supernatants was performed using the Quantikine IL-8 immunoassay (R&D Systems) according to the manufacturer's instructions. Cells were treated as described for the luciferase reporter assay. Before harvesting the cells for the luciferase assay, supernatants (each treatment in triplicate) were frozen and kept at −20 °C until the assay was performed. Thawed samples and IL-8 standard dilutions (50 μl) were added to the provided IL-8 monoclonal antibody-coated microtiter plate containing 100 μl of assay diluent buffer. An enzyme-linked polyclonal antibody was added, and the plates were incubated at room temperature for 2.5 h. After six washes, a substrate solution was added, plates were incubated for 30 min, a stop solution was added, and optical densities were determined by measuring absorbance at 450 nm using a Thermo Max Microplate Reader using Softmax software (Molecular Devices). Using an IL-8 standard curve, IL-8 concentrations in the supernatants were calculated. Data shown are average ± S.E. of triplicate measurements.

Confocal Microscopy—COS-1 cells were plated in 9.6-cm^2 dishes containing glass bottoms (MatTek Corp., 1.5×10^5 cells/dish). One day later, 1 μg of DNA was transfected using the Fugene method, and the next day cells were studied by confocal microscopy. Cells were observed using a Leica TCS-4D confocal laser-scanning microscope, equipped with a Uniphase argon gas laser, using a Plan-Apochromat ×63 water immersion objective (1.4 numeric aperture). Cells expressing YFP-tagged proteins were excited at 488 nm, and emission was collected using a 525 ± 25-nm band pass filter.

FRAP—For determining the mobility of YFP-tagged proteins, FRAP was performed as described previously (6) with minor modifications. Images were taken every 290.3 ms at a resolution of 128 × 128 pixels. After the first image, two consecutive images were taken of a selected square region of fixed size in the nucleus using maximal laser power (0.8 milliwatt, measured at the objective), resulting in bleaching of the fluorescent molecules in this region. Average fluorescence intensity per pixel in the bleached region and in the total nucleus was determined at every time point using Leica Confocal Software (available on the World Wide Web at www.leica-microsystems.com/Confocal_Microscopes). In each experiment, at least 10 cells per condition were analyzed (see Fig. 4*B*). To correct for differences in expression level between individual cells, fluorescence data for the bleached region and the total nucleus were normalized to the prebleaching level. At all time points, data were normalized to the fluorescence in the total nucleus in order to correct for the loss in fluorescence due to the bleach pulse and the imaging (see Fig. 4*C*). Using these data, the $t_{1/2}$ of maximal recovery was determined, which is defined as the time point after bleaching at which the normalized fluorescence has increased to half the amount of the maximal recovery. Every $t_{1/2}$ shown is an average ± S.E. of at least three experiments.

Analysis of Intranuclear Protein Distribution—A previously described method for quantitating the randomness of protein distribution in the nucleus was used (9). Images of trans-

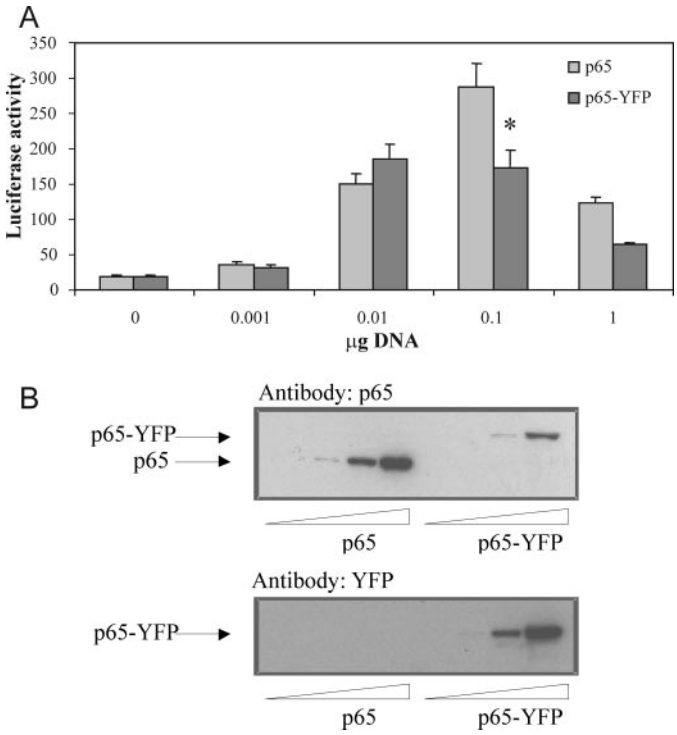

FIGURE 1. **Characterization of p65-YFP.** *A*, transactivation assay. p65 and p65-YFP were transfected into COS-1 cells together with a reporter construct containing a luciferase gene driven by a κB site-containing promoter. Luciferase activity was measured 24 h after transfection. The YFP tag affects transactivational properties of p65 only at maximal induction. *, a statistically significant difference from p65 at same amount of transfected DNA ($p < 0.05$). *B*, Western blots. Protein samples from p65- or p65-YFP-transfected COS-1 cells were analyzed by Western blotting using a p65 antibody (*top panel*) or an YFP antibody (*bottom panel*).

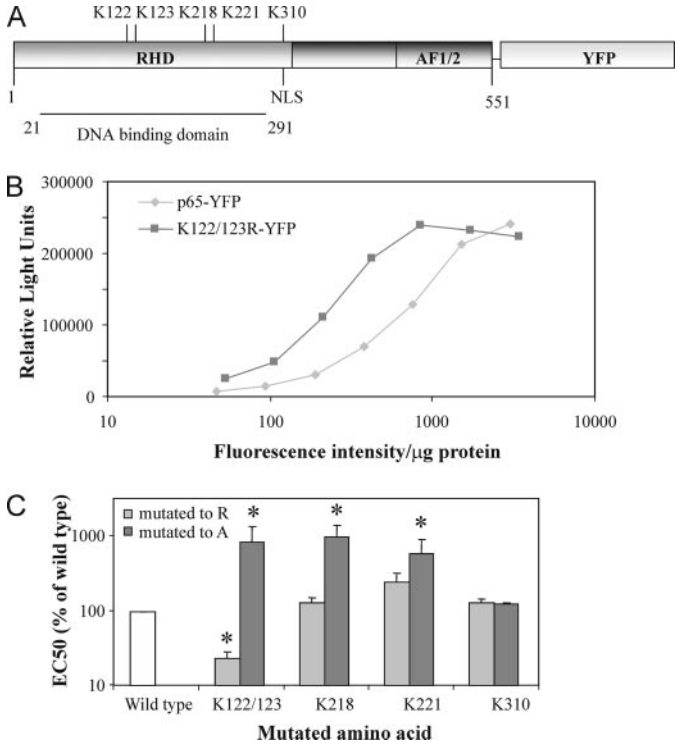

FIGURE 2. *A*, schematic representation of the p65-YFP fusion protein. Five acetylation sites in the DNA-binding domain are indicated as well as the Rel homology domain (*RHD*), the activating function 1/2 domain (*AF1/2*), and the nuclear localization signal (*NLS*). *B*, measuring DNA binding affinity using an ELISA-based method. Luminescence levels were plotted against the relative fluorescence intensity level in the nuclear extracts used. A representative curve for p65-YFP and K122/123R-YFP is shown. From this curve, the fluorescence intensity level at which the luminescence is half-maximal (EC_{50}) can be determined. *C*, relative EC_{50} values (as percentage of wild type) for acetylation mutants of p65-YFP. *, a statistically significant difference from wild type p65-YFP ($p < 0.05$).

fected cells were taken at a resolution of 512 × 512 pixels and analyzed using the program ImageJ (developed at the National Institutes of Health and available on the World Wide Web at rsb.info.nih.gov/ij/). Fluorescence intensity levels were measured on individual points along a line through the nucleus (maximal in length without touching a nucleolus). From all individual measurements along this line, an S.D. and average could be calculated. The quotient of these numbers (the coefficient of variation (CV)) was used as a measure for the degree of randomness of nuclear distribution. In each experiment, at least 10 cells were chosen randomly, and the results were averaged.

Statistical Analysis—Statistical analysis was performed by one-way or two-way ANOVA. Where ANOVA indicated statistical significance, the Bonferroni post hoc test was used to compare individual groups. This test was done using the GraphPad online calculator (available on the World Wide Web at www.graphpad.com/quickcalcs/posttest1.cfm) (see also Ref. 31). Statistical significance was accepted at $p < 0.05$.

RESULTS

Characterization of p65-YFP

In the present study, a fusion protein was used consisting of the NF-κB subunit p65 C-terminally tagged with YFP. Construction of this p65-YFP fusion protein has previously been described (26). First, the activity of this construct on an NF-κB-responsive promoter was studied. The results are shown in Fig. 1*A*. Endogenous p65 does not significantly induce transactivation of this promoter (due to inactivation by endogenous IκB), but overexpression of p65 results in considerable induction. Maximum induction (approximately 15-fold) is reached with transfection of 0.1 μg of plasmid. Induction by the tagged protein is comparable, but the maximum is slightly lower. Subsequently, protein samples were extracted from the nuclei, and Western blots were performed using antibodies against p65 or YFP (Fig. 1*B*). Using the p65 antibody, single bands of the expected size were detected for both p65 and p65-YFP-transfected cells. The YFP antibody stained one major band in p65-YFP transfected cells, indicating that virtually all yellow fluorescence observed in the nucleus is emitted from the full-length intact p65-YFP.

Acetylation Site Mutants of p65-YFP

In Vitro DNA Binding Analysis—A schematic representation of the p65-YFP fusion protein is shown in Fig. 2*A*. Five acetylation sites in the DNA-binding domain are indicated. Two pairs of sites are grouped together (lysines 122/123 and 218/221). Because Lys-122 and Lys-123 have been shown to share a similar function (23), they were mutated simultaneously in the same construct. Because some mutations of Lys-221 are very disruptive to the localization and function of p65, we decided to

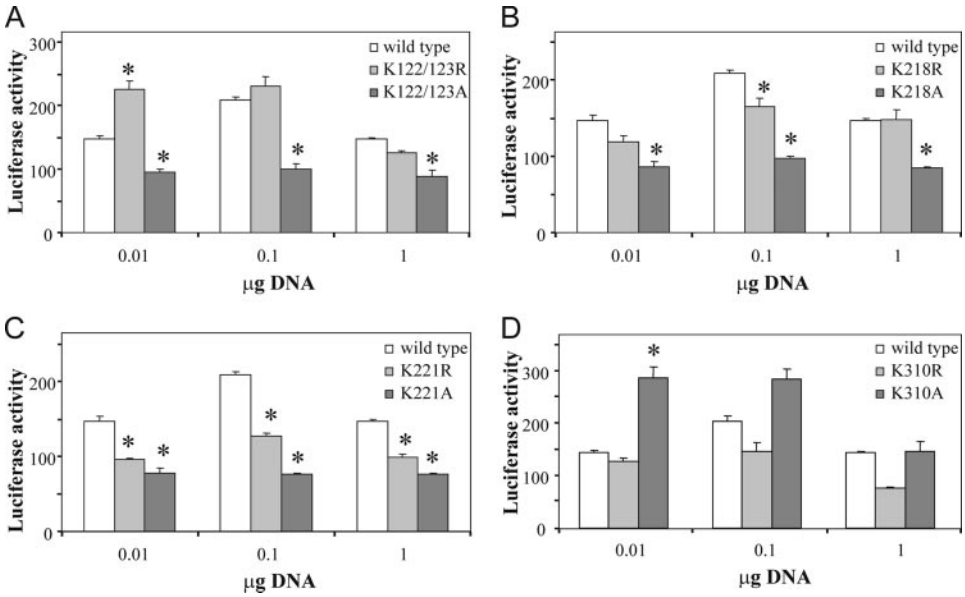

FIGURE 3. **Transactivation assay for p65-YFP acetylation mutants.** Luciferase assays were performed by transfecting the mutants into COS-1 cells together with a κB-luciferase reporter construct. Twenty-four hours later, luciferase activity was measured for K122R/K123R and K122A/K123A (*A*), K218R and K218A (*B*), K221R and K221A (*C*), and K310R and K310A (*D*). *, a statistically significant difference from wild type p65-YFP at same amount of transfected DNA ($p < 0.05$). The wild type data are identical for each *subpanel* and repeatedly shown for better comparison with the mutants.

make single mutants of Lys-218 and Lys-221. All five lysines were mutated to arginine and alanine in p65-YFP. Mutation to arginine retains the positive charge of the amino acid, whereas mutation to alanine neutralizes this charge, thereby mimicking this aspect of acetylation of the lysine residues.

It has been demonstrated that mutation of acetylation sites in p65 alters its DNA binding affinity (23–25). In order to investigate these alterations, the DNA binding affinity of the different mutants was determined *in vitro* using an ELISA-based method. COS-1 cells were transfected with wild type or mutant p65-YFP expression vectors. Nuclear extracts were prepared, and Western blots were performed to determine the integrity of the p65-YFP fusion proteins. The Western blots showed identical bands for wild type p65-YFP (as shown in Fig. 1*B*) and all eight mutants (data not shown).

Subsequently, aliquots of the nuclear extracts were administered to plates coated with oligonucleotides containing a κB response element. Detection of oligonucleotide-bound p65 was performed using a primary p65 antibody, a horseradish peroxidase-conjugated secondary antibody, and a chemiluminescence-based assay. Dilution ranges were made for nuclear extracts, and luminescence was measured for all dilutions. In order to measure relative p65-YFP protein levels, the yellow fluorescence in the nuclear extracts was measured. Subsequently, the luminescence levels were plotted against the relative protein concentrations in the nuclear extract. Representative curves for p65-YFP and K122R/K123R-YFP are shown in Fig. 2*B*. Clearly, the K122R/K123R curve is shifted to the left as compared with the p65-YFP curve, indicating a higher DNA binding affinity of the mutant. From this curve, the concentration at which the luminescence is half-maximal (EC_{50}) can be determined. In each experiment, the EC_{50} for the wild type construct was set at 100%, and all other values were converted accordingly. The observed EC_{50} values are shown in Fig. 2*C*. Mutant K122R/K123R displays a relatively low EC_{50} (23.3 ± 4.6%), reflecting an increased DNA binding affinity. Increased EC_{50} values were observed for the alanine mutants K122A/K123A, K218A, K221A (877.9 ± 519.0, 1016.4 ± 456.9, and 612.4 ± 313.7%, respectively). The alanine mutant K310A, however, displayed an EC_{50} value comparable with that of the wild type, like K310R, K221R, and K218R.

These results are largely in line with findings from EMSAs in earlier reports (23–25), a technique that has been shown to be at least 10 times less sensitive than the ELISA-based technique used in the present study (32). In the EMSA studies, unchanged binding affinity was observed for K218R and K310R (as in our study). The absence of DNA binding was reported for mutants K221R (24) and K122A/K123A (23), indicating that the affinity of these mutants was below the detection limit of EMSA. In our ELISA-based study, the DNA binding affinity could be quantitated, and a decrease in DNA binding (2.5 and 8.8 times, respectively) was observed. In addition, the ~3-fold increase in binding affinity observed for K122R/K123R in the present study was not detected by EMSA (23).

Luciferase Reporter Assays—In order to characterize the functionality of these mutants, reporter assays were performed by transfecting the mutants into COS-1 cells together with a κB-luciferase reporter construct. The results are shown in Fig. 3, *A–D*. Mutation of Lys-122/123 to arginine resulted in increased DNA binding affinity (Fig. 2*C*), and this was reflected in an increased transcriptional activity, which was observed at 0.01 μg of transfected DNA. Mutation to alanine resulted in an inverted effect, a significant loss in DNA binding activity that is reflected in a decrease in transcriptional activity. This effect of mutating Lys-122/123 on transcriptional activity was previously shown by Kiernan *et al.* (23).

Mutation of Lys-218 to arginine did not have a significant effect on DNA binding affinity (Fig. 2*C*), but did show a slight decrease in transcriptional activity after transfection of 0.1 μg of DNA. Mutation of Lys-218 to alanine resulted in a significant decrease in DNA binding affinity, which was reflected in a decreased transcriptional activity. A similar result was found for mutants K221R and K221A. Mutation of Lys-310 to arginine, which was shown not to alter DNA binding affinity, did not result in any significant changes in transcriptional activity. However, mutation to alanine, which does not affect DNA binding affinity either, results in increased transcriptional activity. It has been suggested that the increased transcriptional activity of K310A is a result of increased coactivator binding (24).

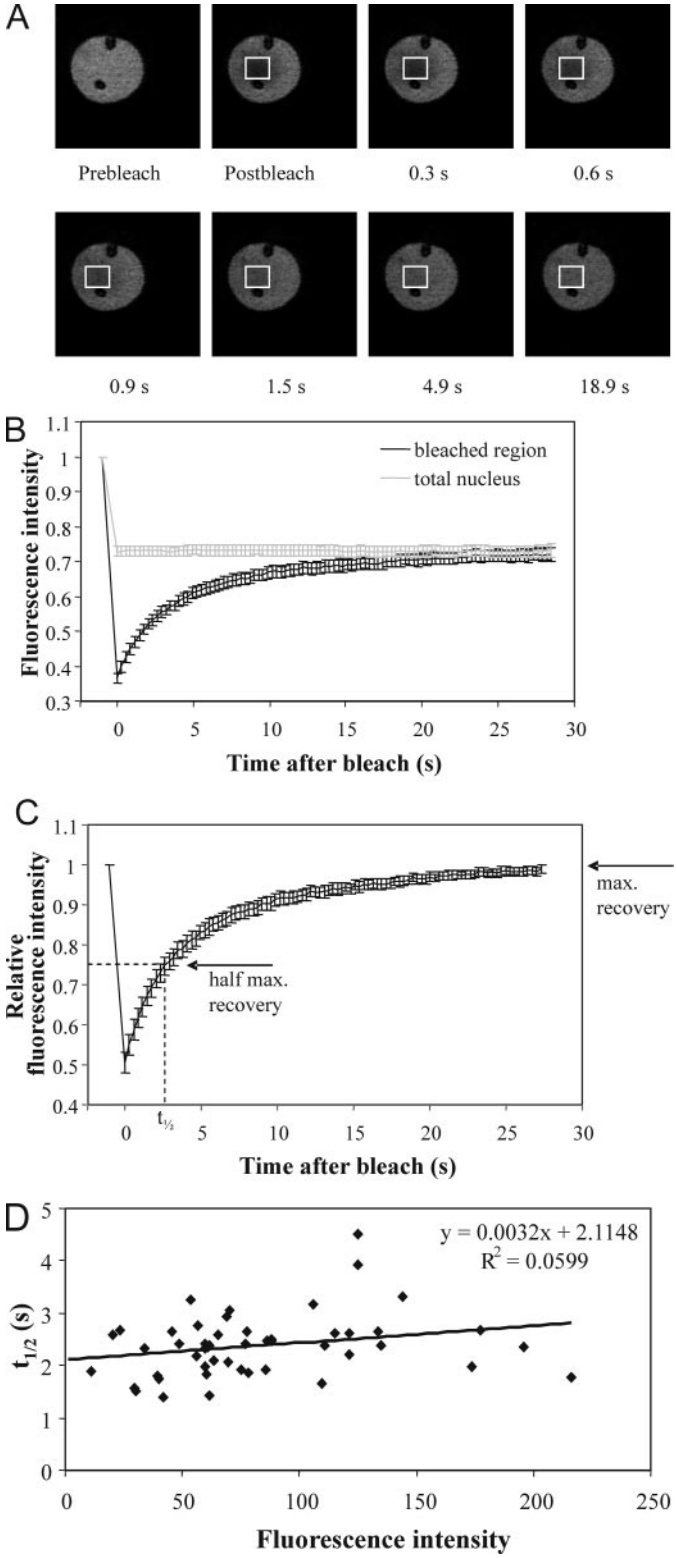

FIGURE 4. **FRAP analysis of p65-YFP.** *A*, COS-1 cells were transfected with p65-YFP (1 μg of DNA/9.6-cm^2 dish). Twenty-four hours after transfection, almost all fluorescence is detected in the nucleus. Maximal laser power is applied to a square region in the nucleus, which causes bleaching of fluorescent molecules present in this region (see *Postbleach image*). Subsequently, the recovery of fluorescence in the bleached area is monitored at different time points after bleaching. *B*, quantitation of FRAP analysis. Fluorescence in the bleached region and the total nucleus was quantitated and plotted against time. *C*, fluorescence in the bleached area corrected for the change in total fluorescence. Using this plot, the $t_{1/2}$ of maximal recovery can be calculated. Each plot shows average values of at least 10 cells. *D*, FRAP analysis was performed on 50 randomly chosen cells from the same batch of p65-YFP-transfected cells in order to test the relationship between mobility and expression level. The $t_{1/2}$ and the fluorescence intensity in the nucleus were plotted for each individual cell.

The transcriptional activities of K218R, K221R, and K310R have been examined in a previous study (24). Surprisingly, a large decrease in activity of K310R was observed in this study, whereas in our studies, this mutant did not show altered transcriptional activity. The reason for this discrepancy is unclear.

In this experiment, the effect of the transfected amount of DNA for the wild type p65-YFP was slightly different from that shown in Fig. 1*A*. The most likely explanation for this discrepancy may be the use of a different batch of COS-1 cells in this series of experiments.

FRAP Analysis—In order to study the relationship between DNA binding affinity and protein mobility, the dynamics of p65-YFP in the nucleus were studied by FRAP. A representative FRAP experiment is shown in Fig. 4*A*. Twenty-four hours after transfection of COS-1 cells with p65-YFP, almost all fluorescence is detected in the nucleus (Fig. 4*A*, *Prebleach image*). Maximal laser power is applied to a square region in the nucleus (~20% of the nuclear area), which causes bleaching of fluorescent molecules present in this region (Fig. 4*A*, *Postbleach image*). Subsequently, the recovery of fluorescence in the bleached area is monitored. The faster this recovery, the higher the mobility of the fluorescent protein.

Subsequently, the fluorescence in the bleached region and in the total nucleus was quantitated. During the bleach pulse, fluorescence in the bleached area decreases to 37% of the level before the pulse. Immediately after the bleach pulse, the fluorescence level starts to increase, until around 20 s, when it has reached a level similar to that of the total nucleus. The fact that the two lines converge indicates that fluorescence recovery is almost complete, reflecting complete exchange of p65-YFP molecules between the bleached region and the rest of the nucleus. It can therefore be concluded that no p65-YFP molecules exist in the nucleus that are immobile during this time frame. To control for the loss of fluorescence in the nucleus due to the bleach pulse and the imaging, we normalized the fluorescence in the bleached area to that of the total nucleus. These normalized data are shown in Fig. 4*C* and were used to determine the $t_{1/2}$ of recovery, which is defined as the time point after bleaching at which the recovery is half-maximal. In these curves, maximal recovery reaches 1 if all molecules are mobile, whereas the existence of a population of molecules that are immobile during the time frame of the experiment results in lower recovery rates.

In order to test if the mobility of p65-YFP was dependent on the number of p65 molecules present in the nucleus, FRAP analysis was performed on 50 randomly chosen cells from the same batch of p65-YFP-transfected cells. Both the $t_{1/2}$ and the fluorescence intensity in the nucleus were measured. For each cell, $t_{1/2}$ was plotted against the fluorescence intensity, and the resulting graph is shown in Fig. 4*D*. This graph shows no correlation between fluorescence intensity and mobility. This result indicates that binding sites for p65 in the nucleus that decrease its mobility are highly abundant and are not saturable by increasing the expression level of p65.

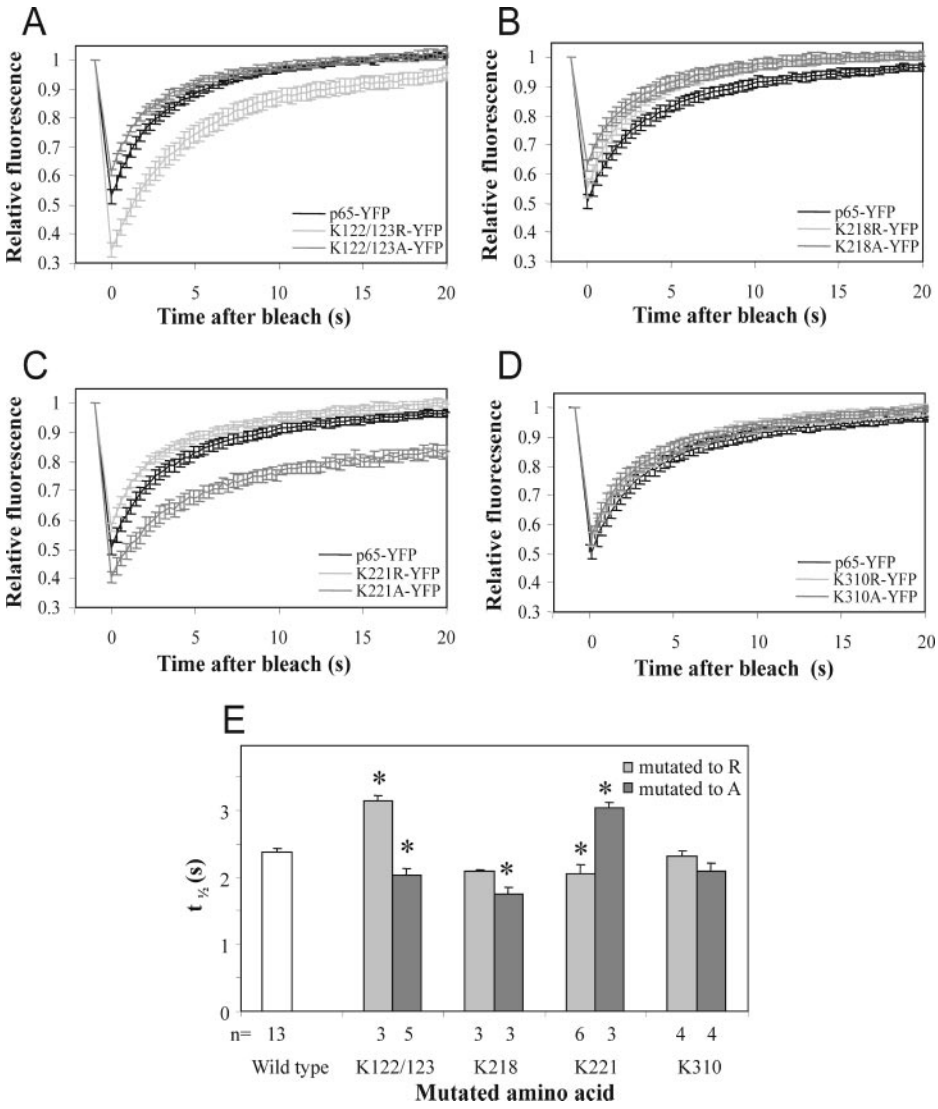

FIGURE 5. **FRAP analysis of p65-YFP acetylation mutants.** FRAP was performed as described in the legend to Fig. 4. Representative FRAP curves for the mutants are shown in *A–D*. Corresponding $t_{1/2}$ values are presented in *E*. *, a statistically significant difference from wild type p65-YFP ($p < 0.05$).

FRAP analysis was performed on wild type p65-YFP and the acetylation mutants. Representative FRAP curves are shown in Fig. 5, *A–D*, and the corresponding $t_{½}$ values are presented in Fig. 5*E*. Two mutants display a lower mobility than the wild type protein, K122R/K123R and K221A. This is reflected by a higher $t_{½}$ (3.34 ± 0.21 and 3.03 ± 0.08 s) as compared with wild type p65-YFP (2.38 ± 0.06 s; see Fig. 5*E*). In addition, a lower fluorescence level immediately after bleaching was observed for these two mutants (Fig. 5, *A* and *C*). This correlation between $t_{½}$ and bleach efficiency is commonly seen in FRAP experiments and is a result of the movement of molecules into and out of the bleached area during the bleach pulse. Mutants K122A/K123A, K218R, K218A, K221R, and K310A all display a slightly higher mobility than the wild type protein, reflected in a lower $t_{½}$ value (2.04 ± 0.10, 1.41 ± 0.11, 1.76 ± 0.10, 2.05 ± 0.13, and 3.03 ± 0.08 s, respectively) (Fig. 5*E*). Mutant K310R shows a mobility similar to the wild type ($t_{½}$ = 2.31 ± 0.07 s, Fig. 5*E*).

Remarkably, 20 s after the bleach pulse, the K122R/K123R (Fig. 5*A*) and the K221A curve (Fig. 5*C*) did not show complete recovery. At the end of the experiment (after 29 s), the K221A curve still did not display complete recovery, but the K122R/K123R curve did show full recovery at this time point (data not shown). This indicates that a subpopulation of the K221A mutant is immobile during this time frame. Images of this mutant show large aggregations of this protein in both nucleus and cytoplasm that are not present in cells expressing any of the other mutants (see Fig. 9). Further analysis of our FRAP images showed that fluorescence in these aggregations does not recover after photobleaching, whereas recovery is observed in the rest of the nucleus. This indicates that the subpopulation that is immobile during the time frame of our experiments is located in the aggregations and that this subpopulation should therefore be considered an artifact of protein aggregation. It has indeed been shown that Lys-221 is involved in intramolecular amino acid contacts (33), which may be relevant to adequate folding of the protein. Mutating this residue may therefore result in protein misfolding. We assume that misfolded proteins form these aggregations, which are of little physiological relevance. K221A was therefore excluded from further analysis.

The $t_{½}$ values of all mutants were plotted against their EC_{50} values, and the resulting graph is shown in Fig. 6. A clear correlation between these two parameters is evident from this graph. A low $t_{½}$ coincides with a high EC_{50}, indicating that a high mobility coincides with a low DNA binding affinity in the nucleus.

p65-YFP and YFP-p65: In Vitro DNA Binding and FRAP Analysis

Subsequently, we studied the effect of moving the YFP tag from the C terminus of p65 to the N terminus, resulting in an YFP-p65 fusion protein. YFP-p65 and p65-YFP were tranfected into COS cells, and their DNA binding affinity was measured using the ELISA-based method described above. The resulting EC_{50} values are shown in Fig. 7*A*. No significant difference was detected between the EC_{50} values of YFP-p65 and p65-YFP, indicating that moving the YFP tag from the C to the N terminus does not affect the DNA binding affinity of the fusion protein.

Since the different DNA binding affinities of the acetylation mutants of p65 were reflected in differences in mobility, we expected the similarity between the affinities of p65-YFP and YFP-p65 to be reflected in their respective mobilities as well. In

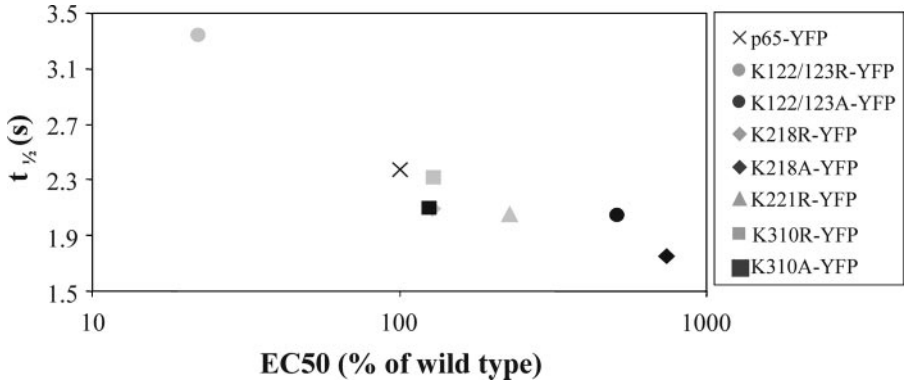

FIGURE 6. **Correlation between mobility and DNA binding.** The $t_{1/2}$ values of wild type and mutant p65-YFP (as shown in Fig. 5*E*) were plotted against their EC_{50} values (as shown in Fig. 2*C* (mutant K221A was excluded from this analysis)). A correlation between these two parameters is evident. Regression analysis by ANOVA indicated a highly significant correlation ($F(1,6) = 19.69$ ($p = 0.004$)).

order to study this, FRAP studies were performed for both constructs, and the resulting $t_{½}$ values are presented in Fig. 7*B*. Surprisingly, YFP-p65 displayed a significantly higher mobility than p65-YFP ($t_{½} = 1.77 \pm 0.05$ and 2.38 ± 0.06 s, respectively). In order to compare these data to the data from the acetylation mutants, the results for YFP-p65 were added to Fig. 6, in which the EC_{50} values were plotted against the respective $t_{½}$ values. The resulting graph is presented in Fig. 7*C*. Clearly, by adding this data point to the plot, the correlation between DNA binding and mobility is significantly reduced, which was quantitated by linear regression analysis (by ANOVA) of the data excluding YFP-p65 ($F(1,6) = 17.58$, $p = 0.0041$) and including YFP-p65 ($F(1,7) = 25.50$, $p = 0.0023$). The DNA binding affinity of YFP-p65 is not significantly different from p65-YFP, whereas its $t_{½}$ value is significantly lower and among the lowest, similar to the affinity of YFP-K218A.

Since mobility is measured *in vivo* and DNA binding is measured *in vitro*, it can be suggested that a possible difference between *in vivo* and *in vitro* DNA binding may explain the observed discrepancy between the observed mobility and DNA binding for YFP-p65. The activity of this construct in a κB-luciferase reporter assay may indicate if *in vivo* DNA binding is intact. Therefore, the activity of YFP-p65 in this assay was studied, and the results are shown in Fig. 8*A*. Surprisingly, YFP-p65 displayed transcriptional activity comparable with that of p65-YFP, indicating that *in vivo* DNA binding to a transiently transfected promoter is intact. In order to investigate if DNA binding of this construct on an endogenous promoter is intact as well, we studied the activity of YFP-p65 and p65-YFP on the induction of IL-8. Surprisingly, YFP-p65 displayed an even higher induction of IL-8 than p65-YFP (Fig. 8*B*), indicating that *in vivo* binding to an endogenous promoter is intact. Two-way ANOVA of the IL-8 assays revealed a significant difference between the two constructs ($F(1,23) = 5.60$, $p = 0.03$) and a significant effect of the DNA concentration ($F(3,23) = 24.16$, $p = 3.5 \times 10^{-7}$).

YFP, p65-YFP, YFP-p65, and Acetylation Site Mutants: Analysis of Intranuclear Distribution

In Fig. 9, pictures are shown of the intranuclear distributions of YFP and several wild type and mutant p65-YFP fusion proteins. Large differences between the distributions of the different proteins were observed. YFP displays a very even distribution. It is present in both cytoplasm and nucleus, and in these compartments its distribution is highly random, apart from being excluded from the nucleoli. The pattern shown by p65-YFP is remarkably different. Its localization is limited to the nucleus (excluded from the nucleoli), and within the nucleus its distribution is less even than that of YFP. There are large areas with a high concentration and small areas with low concentration of this protein. Mutant K122A/K123A-YFP shows a distribution pattern that is more even than that of wild type p65-YFP although less uniform than YFP. Even more uneven than the distribution pattern of p65-YFP is that of K122R/K123R-YFP. This protein also shows exclusion from the nucleolus and small areas with low receptor concentration like p65-YFP, but in addition it appears to distribute in small discrete focal domains, giving its distribution a speckled pattern. A more pronounced speckled pattern is shown by K221A-YFP, but these focal domains are fewer in number and larger and are probably the result of protein aggregation as mentioned before. The distribution of the N-terminally tagged YFP-p65 was remarkably more even than that of p65-YFP and resembles that of K122A/K123A-YFP.

Distributions similar to that of K122A/K123A-YFP are found for mutants K218R-YFP, K218A-YFP, and K221R-YFP, whereas mutants K310R-YFP and K310A-YFP displayed a distribution similar to wild type p65-YFP (data not shown). The acetylation mutant of YFP-p65, mutant YFP-K122R/K123R showed a more speckled distribution (data not shown), reminiscent of its C-terminally tagged analogue. YFP-K122/123A showed a highly random distribution (data not shown), similar to that of YFP-p65.

These different distributions were quantitated as described previously (9). A line was drawn through the nucleus, maximal in length without touching a nucleolus. For every pixel along this line, fluorescence intensities were measured. The average fluorescence intensity and the S.D. were measured, and their quotient (the CV) was determined. This CV is a measure of the randomness of the distribution. The higher the CV, the more nonrandom the distribution is. The qualitative differences in distributions that were described above were reflected in the detected CV values. Wild type p65-YFP had a CV of 0.11 ± 0.01. The mutants with more nonrandom distributions, K122A/K123A and K221A showed a significantly higher CV (0.16 ± 0.01 and 0.33 ± 0.03, respectively). The other mutants had CV values that ranged between 0.09 ± 0.01 (K218A) and 0.11 ± 0.01 (K310A). Previously, it has been shown that distribution and mobility of the glucocorticoid receptor are linked (9). In order to investigate if this correlation can be extended to other transcription factors, $t_{½}$ values were plotted against CV values. The resulting graph is shown in Fig. 9*B*, and from this graph it is

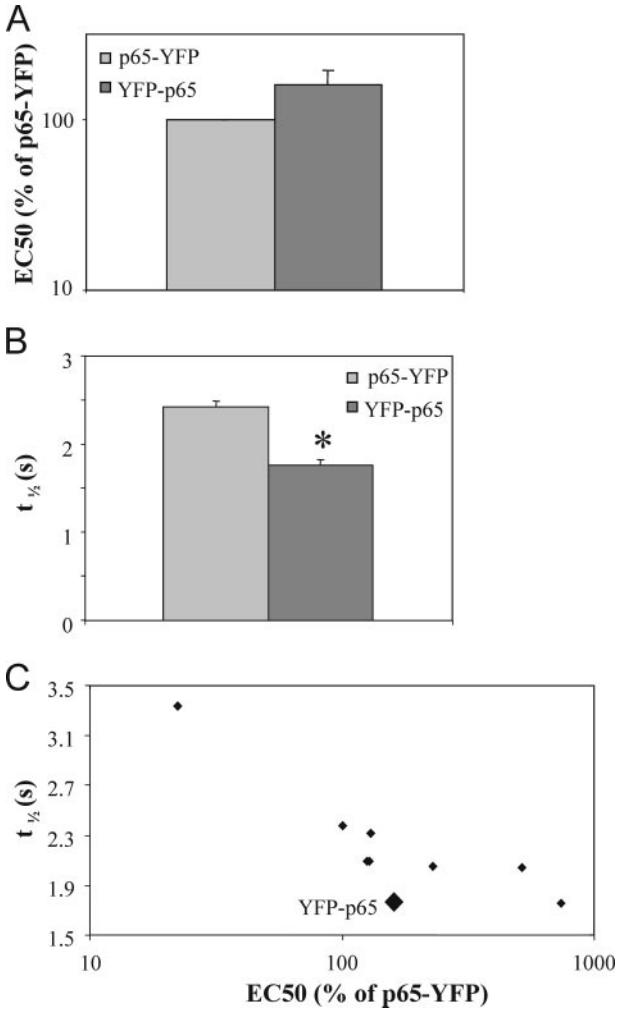

FIGURE 7. **p65-YFP and YFP-p65.** *A*, *in vitro* DNA binding analysis. DNA binding affinities for p65-YFP and YFP-p65 were measured as described in the legend to Fig. 2. No significant difference was detected. *B*, FRAP analysis of p65-YFP and YFP-p65. FRAP was performed as described in the legend to Fig. 4, and $t_{1/2}$ values are presented. A lower $t_{1/2}$ was detected for YFP-p65, indicating a higher intranuclear mobility. *, a statistically significant difference from p65-YFP ($p < 0.05$). *C*, correlation between mobility and DNA binding. Data from YFP-p65 were added to the plot shown in Fig. 6. The correlation between mobility and DNA binding is significantly reduced.

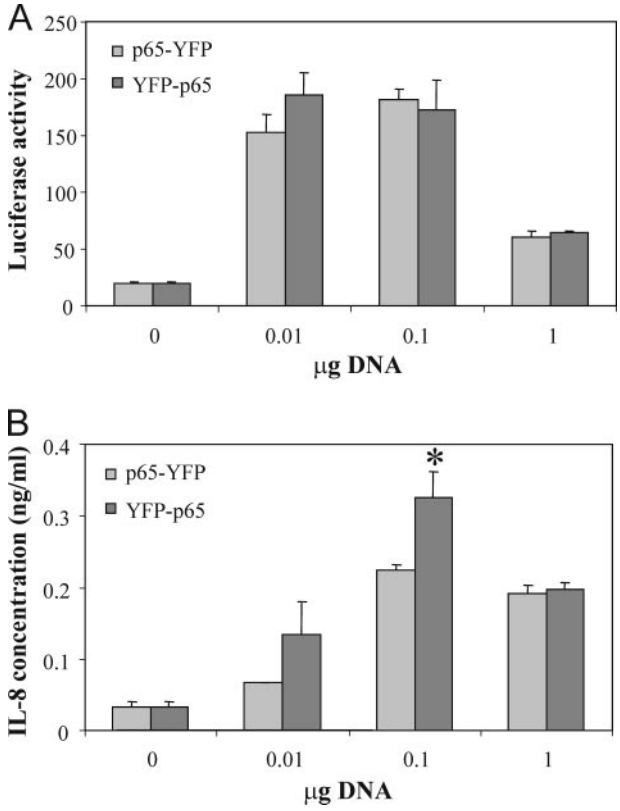

FIGURE 8. **Transactivational properties of YFP-p65.** *A*, luciferase assay performed as described in the legend to Fig. 1*A*. No statistically significant difference was observed between p65-YFP and YFP-p65. *B*, IL-8 assay. IL-8 concentration was measured by ELISA 24 h after transfection of p65-YFP or YFP-p65 in COS-1 cells. *, a statistically significant difference from p65-YFP ($p < 0.05$).

clear that there is a positive correlation between CV and $t_{½}$ ($r^2 = 0.9223$). Linear regression analysis shows a highly significant correlation ($F(1,10) = 117.82$ ($p = 7.46 \times 10^{-7}$). The higher the CV, the higher the $t_{½}$ and *vice versa*, indicating that a random distribution coincides with a high mobility and *vice versa*. Since these results are in line with previous findings for the glucocorticoid receptor (9), we suggest that this is a general rule for transcription factors in the nucleus.

DISCUSSION

In the present study, we have investigated if DNA binding affinity is a determinant of intranuclear mobility of transcription factors. For the first time, a series of point mutants of a transcription factor covering a range of DNA binding affinities (higher and lower than the wild type) was used to study the correlation between DNA binding affinity and mobility. By studying eight different mutations of acetylation sites in the NF-κB subunit p65, a negative correlation between DNA binding affinity and intranuclear mobility was observed. This was in line with earlier studies of DNA binding-deficient mutants of GR (6), androgen receptor (8), and Acep1 (15), which all show a dramatic increase in mobility as compared with the wild type protein. It can be concluded that specific DNA binding is a major determinant of the intranuclear mobility of p65.

The DNA binding data shown in the present paper represent binding to the κB site of the immunoglobulin light chain gene promoter. The crystal structure of a p65-p50 heterodimer bound to this sequence has been resolved, and it appears that four lysine residues that were mutated in the present study (Lys-122, Lys-123, Lys-218, and Lys-221) contact phosphate groups in the DNA backbone (21). The fifth lysine mutated in the present study (Lys-310) is not involved in DNA binding. All four DNA-contacting lysines are conserved between p65 and p50. The positions of these residues appear to be similar in p65 and p50 homodimers and in p65/p50 heterodimers upon binding to their respective consensus site, indicating that binding of these residues is not dependent on the DNA sequence. This was further demonstrated by crystallizing the p65 homodimer bound to different DNA targets. Whereas the position of several amino acids in the DNA-binding region of p65 was highly dependent on the DNA target, the position of the four lysine residues contacting the phosphate backbone was independent of the DNA target sequence (34). It can therefore be suggested that alterations in DNA binding after substitution of one of these four lysine residues is not restricted to the κB site of the

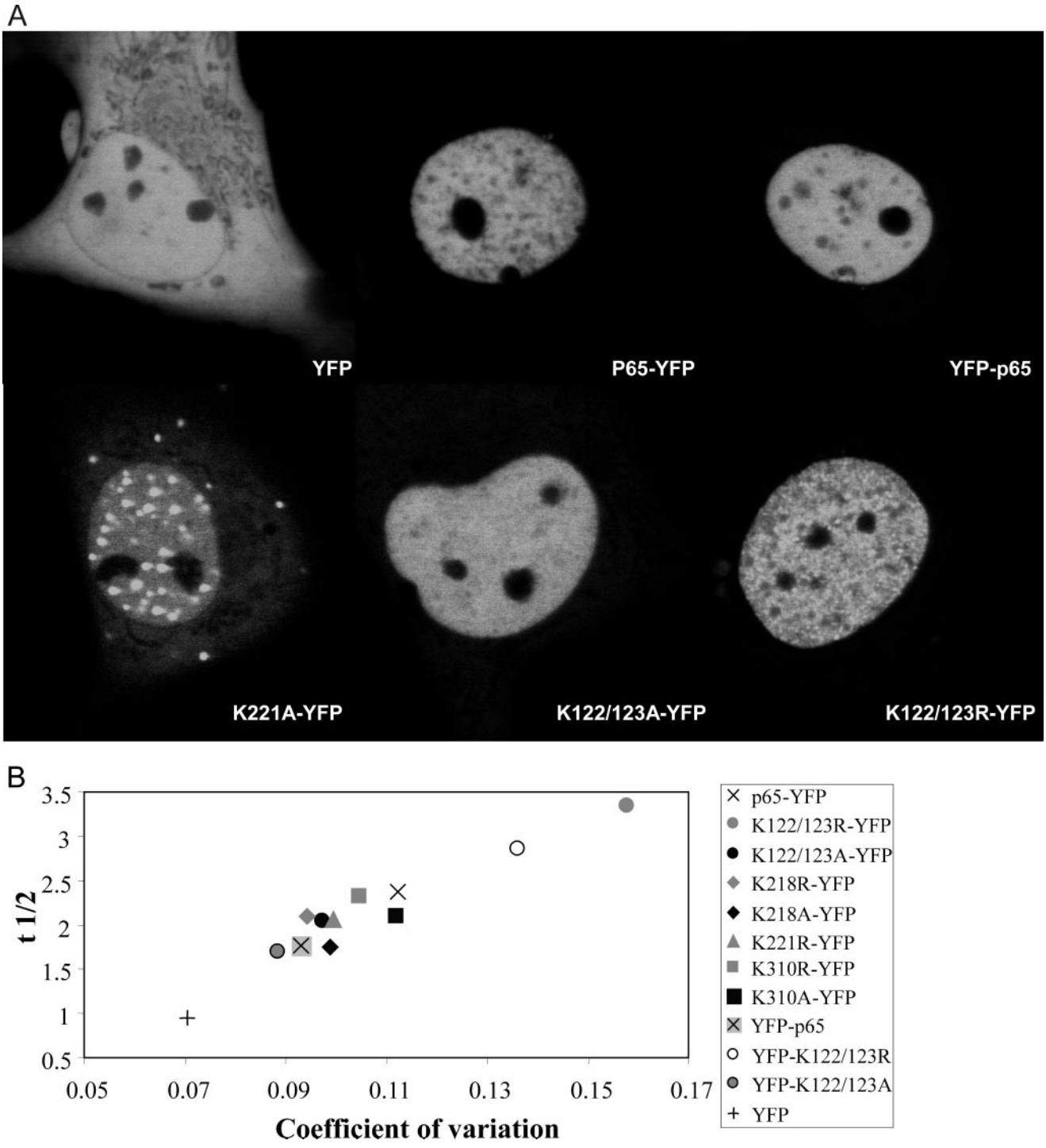

FIGURE 9. **Analysis of intranuclear distribution.** *A*, representative images of the intranuclear distributions of YFP and several wild type and mutant p65-YFP fusion proteins. A large variation exists between the distributions of the different proteins. Distribution of p65-YFP is limited to the nucleus (excluded from the nucleoli), and within the nucleus its distribution is a lot less random than that of YFP. Even more nonrandom than the distribution pattern of p65-YFP is the one of K122/123R-YFP. The distribution of the N-terminally-tagged YFP-p65 was remarkably more random than that of p65-YFP and resembles K122A/K123A-YFP. A more pronounced speckled pattern is shown by K221A-YFP. *B*, correlation between intranuclear mobility and distribution. Intranuclear distributions were quantitated as follows. A line was drawn through the nucleus, and along this line fluorescence intensities were measured. The average fluorescence intensity and the S.D. value were measured. Their quotient (the CV) is a measure for the randomness of the distribution. The higher the CV, the more nonrandom the distribution. The $t_{1/2}$ values as measured by FRAP were plotted against the CV values (mutant K221A was excluded from this analysis). A positive correlation between CV and $t_{1/2}$ ($r^2 = 0.9223$) was observed. Regression analysis shows a highly significant correlation ($F(1,10) = 117.82$ ($p = 7.46 \times 10^{-7}$).

immunoglobulin gene but that these data can at least be extrapolated to other κB sequences.

All changes in DNA binding affinity of p65 observed in this study are reflected in changes in mobility, but the difference in mobility between YFP-p65 and p65-YFP cannot be explained by an alteration in DNA binding affinity. Moving the YFP-tag from the C terminus to the N terminus increased the mobility of the fusion protein dramatically but did not result in a signif-

icant change in DNA binding affinity or transcriptional activity on a transfected or endogenous promoter. Interestingly, altering the DNA binding affinity of YFP-p65 by mutating acetylation sites shows mobility changes similar to those observed for the p65-YFP mutants (data not shown), indicating that DNA binding is intact and still a determinant of intranuclear mobility.

Several explanations exist for the difference in mobility between YFP-p65 and p65-YFP. First, there may be a difference in the ability to interact indirectly with DNA through association with proteins or protein complexes that directly bind DNA. For example, it has been shown that p65 can physically interact with the glucocorticoid receptor, thereby inhibiting its function. Changing the YFP tag from the C to N terminus may have altered the affinity for this type of interaction, thereby changing the association rate of p65 to DNA. Unfortunately, these changes cannot be observed by studying binding to or activation of κB consensus sites. Second, interaction of p65 with proteins affecting the DNA binding affinity of p65 may have been altered. For example, interaction with the inhibitor protein IκB has been shown to decrease the DNA binding affinity of p65 (35). For other transcription factors, similar effects of association with other proteins have been observed. FRAP analysis of the transcription factor interferon regulatory factor 8 (36) shows decreased mobility after introduction of partner proteins, but this effect is absent after mutation of its DNA-binding domain, indicating altered DNA binding upon introduction of these partner proteins. Deletion of coactivator-binding domains in the glucocorticoid receptor (6) or CREB (37) significantly reduces intranuclear mobility of these transcription factors. Third, it could be suggested that interaction with chromatin *in vivo*, including possible interactions with histone tails, may be different between YFP-p65 and p65-YFP. Since we measured DNA binding *in vitro* in the absence of histone proteins, this explanation cannot be excluded.

In addition, we found a positive correlation between the randomness of nuclear distribution and mobility. As previously observed for several other transcription factors (4, 9, 38–41), p65-YFP distributes in focal domains, resulting in a punctate distribution. The more punctate the distribution of the p65-YFP acetylation mutant, the lower its mobility. This correlation has previously been shown for GR (9), so it appears to extend to transcription factors in general. In contrast to the correlation between DNA binding and mobility, this correlation was not lost after moving the YFP tag from the C to the N terminus.

The correlation between distribution and mobility indicates that sites at which transcription factors associate in the nucleus are not randomly distributed over the nucleus. Since we have shown that DNA binding affinity is a significant determinant for intranuclear mobility of a transcription factor, the distribution into areas with high and low receptor concentration is probably determined by differences in DNA binding as well. Several factors may determine these local differences. First, since it has been shown that 35% of the DNA-binding sites of p65 contain a canonical κB site (11), the distribution of these sites is probably a major determinant of p65 nuclear distribution. Second, the interaction with other nuclear proteins may play a role. This type of interaction may target transcription factors to specific sites or may alter the specificity of the DNA binding of the transcription factor, or these proteins may be able to bind to specific DNA sequences themselves. The relevance of these protein-protein interactions was supported by our data on YFP-p65 and p65-YFP. Third, differences in the condensation state of the chromatin and therefore local DNA accessibility may determine the association rate of a transcription factor with DNA and thus its distribution.

Acknowledgments—We thank Dr. Onno Meijer and Iain Uings for helpful discussion.

REFERENCES

1. Houtsmuller, A. B., Rademakers, S., Nigg, A. L., Hoogstraten, D., Hoeijmakers, J. H., and Vermeulen, W. (1999) *Science* **284,** 958–961
2. Phair, R. D., and Misteli, T. (2000) *Nature* **404,** 604–609
3. Stenoien, D. L., Patel, K., Mancini, M. G., Dutertre, M., Smith, C. L., O'Malley, B. W., and Mancini, M. A. (2001) *Nat. Cell Biol.* **3,** 15–23
4. Stenoien, D. L., Mancini, M. G., Patel, K., Allegretto, E. A., Smith, C. L., and Mancini, M. A. (2000) *Mol. Endocrinol.* **14,** 518–534
5. Stenoien, D. L., Nye, A. C., Mancini, M. G., Patel, K., Dutertre, M., O'Malley, B. W., Smith, C. L., Belmont, A. S., and Mancini, M. A. (2001) *Mol. Cell. Biol.* **21,** 4404–4412
6. Schaaf, M. J., and Cidlowski, J. A. (2003) *Mol. Cell. Biol.* **23,** 1922–1934
7. Sprague, B. L., Pego, R. L., Stavreva, D. A., and McNally, J. G. (2004) *Biophys. J.* **86,** 3473–3495
8. Farla, P., Hersmus, R., Geverts, B., Mari, P. O., Nigg, A. L., Dubbink, H. J., Trapman, J., and Houtsmuller, A. B. (2004) *J. Struct. Biol.* **147,** 50–61
9. Schaaf, M. J., Lewis-Tuffin, L. J., and Cidlowski, J. A. (2005) *Mol. Endocrinol.* **19,** 1501–1515
10. Phair, R. D., Scaffidi, P., Elbi, C., Vecerova, J., Dey, A., Ozato, K., Brown, D. T., Hager, G., Bustin, M., and Misteli, T. (2004) *Mol. Cell. Biol.* **24,** 6393–6402
11. Martone, R., Euskirchen, G., Bertone, P., Hartman, S., Royce, T. E., Luscombe, N. M., Rinn, J. L., Nelson, F. K., Miller, P., Gerstein, M., Weissman, S., and Snyder, M. (2003) *Proc. Natl. Acad. Sci. U. S. A.* **100,** 12247–12252
12. Euskirchen, G., Royce, T. E., Bertone, P., Martone, R., Rinn, J. L., Nelson, F. K., Sayward, F., Luscombe, N. M., Miller, P., Gerstein, M., Weissman, S., and Snyder, M. (2004) *Mol. Cell. Biol.* **24,** 3804–3814
13. Bieda, M., Xu, X., Singer, M. A., Green, R., and Farnham, P. J. (2006) *Genome Res.* **16,** 595–605
14. Cawley, S., Bekiranov, S., Ng, H. H., Kapranov, P., Sekinger, E. A., Kampa, D., Piccolboni, A., Sementchenko, V., Cheng, J., Williams, A. J., Wheeler, R., Wong, B., Drenkow, J., Yamanaka, M., Patel, S., Brubaker, S., Tammana, H., Helt, G., Struhl, K., and Gingeras, T. R. (2004) *Cell* **116,** 499–509
15. Karpova, T. S., Chen, T. Y., Sprague, B. L., and McNally, J. G. (2004) *EMBO Rep.* **5,** 1064–1070
16. Baldwin, A. S., Jr. (2001) *J. Clin. Invest.* **107,** 3–6
17. Baldwin, A. S., Jr. (1996) *Annu. Rev. Immunol.* **14,** 649–683
18. Ganchi, P. A., Sun, S. C., Greene, W. C., and Ballard, D. W. (1993) *Mol. Cell. Biol.* **13,** 7826–7835
19. Chen, L. F., and Greene, W. C. (2003) *J. Mol. Med.* **81,** 549–557
20. Greene, W. C., and Chen, L. F. (2004) *Novartis Found. Symp.* **259,** 208–217
21. Chen, F. E., Huang, D. B., Chen, Y. Q., and Ghosh, G. (1998) *Nature* **391,** 410–413
22. Chen, Y. Q., Ghosh, S., and Ghosh, G. (1998) *Nat. Struct. Biol.* **5,** 67–73
23. Kiernan, R., Bres, V., Ng, R. W., Coudart, M. P., El Messaoudi, S., Sardet, C., Jin, D. Y., Emiliani, S., and Benkirane, M. (2003) *J. Biol. Chem.* **278,** 2758–2766
24. Chen, L. F., Mu, Y., and Greene, W. C. (2002) *EMBO J.* **21,** 6539–6548
25. Chen, L., Fischle, W., Verdin, E., and Greene, W. C. (2001) *Science* **293,** 1653–1657
26. Garside, H., Stevens, A., Farrow, S., Normand, C., Houle, B., Berry, A., Maschera, B., and Ray, D. (2004) *J. Biol. Chem.* **279,** 50050–50059

27. Nelson, G., Wilde, G. J., Spiller, D. G., Kennedy, S. M., Ray, D. W., Sullivan, E., Unitt, J. F., and White, M. R. (2003) *J. Cell Sci.* **116,** 2495–2503
28. Ruben, S. M., Dillon, P. J., Schreck, R., Henkel, T., Chen, C. H., Maher, M., Baeuerle, P. A., and Rosen, C. A. (1991) *Science* **251,** 1490–1493
29. Schmid, R. M., Perkins, N. D., Duckett, C. S., Andrews, P. C., and Nabel, G. J. (1991) *Nature* **352,** 733–736
30. Andrews, N. C., and Faller, D. V. (1991) *Nucleic Acids Res.* **19,** 2499
31. Hsu, J. C. (1996) *Multiple Comparisons: Theory and Methods*, p. 13, Chapman and Hall, London, UK
32. Renard, P., Ernest, I., Houbion, A., Art, M., Le Calvez, H., Raes, M., and Remacle, J. (2001) *Nucleic Acids Res.* **29,** E21
33. Huxford, T., Huang, D. B., Malek, S., and Ghosh, G. (1998) *Cell* **95,** 759–770
34. Chen, Y. Q., Sengchanthalangsy, L. L., Hackett, A., and Ghosh, G. (2000) *Structure* **8,** 419–428
35. Zabel, U., and Baeuerle, P. A. (1990) *Cell* **61,** 255–265
36. Laricchia-Robbio, L., Tamura, T., Karpova, T., Sprague, B. L., McNally, J. G., and Ozato, K. (2005) *Proc. Natl. Acad. Sci. U. S. A.* **102,** 14368–14373
37. Mayr, B. M., Guzman, E., and Montminy, M. (2005) *J. Biol. Chem.* **280,** 15103–15110
38. van Steensel, B., Brink, M., van der, M. K., van Binnendijk, E. P., Wansink, D. G., de Jong, L., de Kloet, E. R., and van Driel, R. (1995) *J. Cell Sci.* **108,** 3003–3011
39. Htun, H., Barsony, J., Renyi, I., Gould, D. L., and Hager, G. L. (1996) *Proc. Natl. Acad. Sci. U. S. A.* **93,** 4845–4850
40. Elbi, C., Misteli, T., and Hager, G. L. (2002) *Mol. Biol. Cell* **13,** 2001–2015
41. Fejes-Toth, G., Pearce, D., and Naray-Fejes-Toth, A. (1998) *Proc. Natl. Acad. Sci. U. S. A.* **95,** 2973–2978

The Relationship between Intranuclear Mobility of the NF-κB Subunit p65 and Its DNA Binding Affinity

Marcel J. M. Schaaf, Lynsey Willetts, Brian P. Hayes, Barbara Maschera, Eleni Stylianou and Stuart N. Farrow

J. Biol. Chem. 2006, 281:22409-22420.
doi: 10.1074/jbc.M511086200 originally published online June 7, 2006
